**Cell Metabolism, Volume *31***

## Supplemental Information

# NTS Catecholamine Neurons Mediate Hypoglycemic Hunger via Medial Hypothalamic Feeding Pathways

**Iltan Aklan, Nilufer Sayar Atasoy, Yavuz Yavuz, Tayfun Ates, Ilknur Coban, Fulya Koksalar, Gizem Filiz, Iskalen Cansu Topcu, Merve Oncul, Pelin Dilsiz, Utku Cebecioglu, Muhammed Ikbal Alp, Bayram Yilmaz, Deborah R. Davis, Karolina Hajdukiewicz, Kenji Saito, Witold Konopka, Huxing Cui, and Deniz Atasoy**

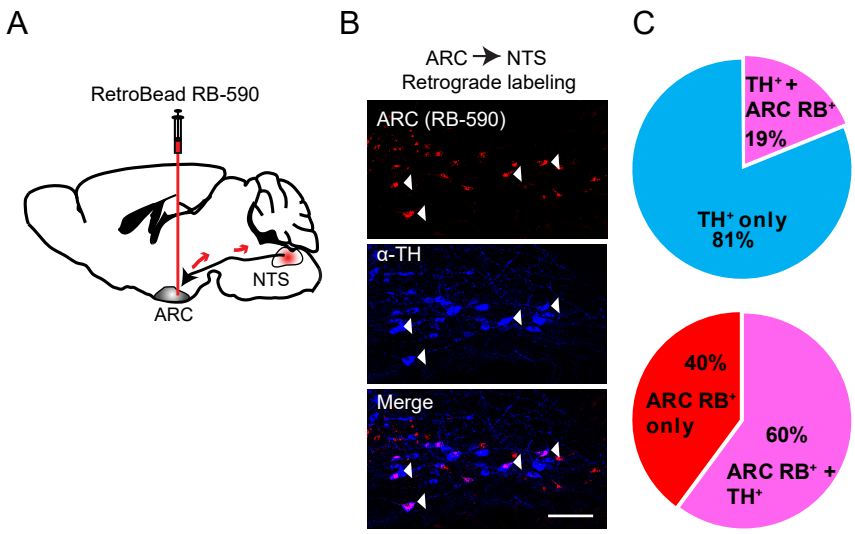


**Figure S1. Quantification of ARC projecting NTS$^{TH}$ neurons** (related to Figure 1)

(A) Schematic for retrograde labeling of ARC projecting NTS neurons by fluorescent beads.

(B) Representative images depicting retrogradely labeled NTS$^{TH}$ neurons (red) using fluorescent beads injected into ARC and anti-TH immunolabeling (blue). Scale: 50 μm

(C) Upper panel: Pie chart showing relative abundance of NTS$^{TH}$ neurons that are retrogradely labeled back from ARC (out of total n=1422 NTS$^{TH}$ neurons, n=270 were retrogradely labeled back from the ARC; counted from 4 mice). Lower panel: Pie chart depicting the fraction of ARC projecting NTS neurons that express TH (out of total n=449 retrogradely labeled NTS neurons, n=270 expressed TH; counted from 4 mice. RB: RetroBead).

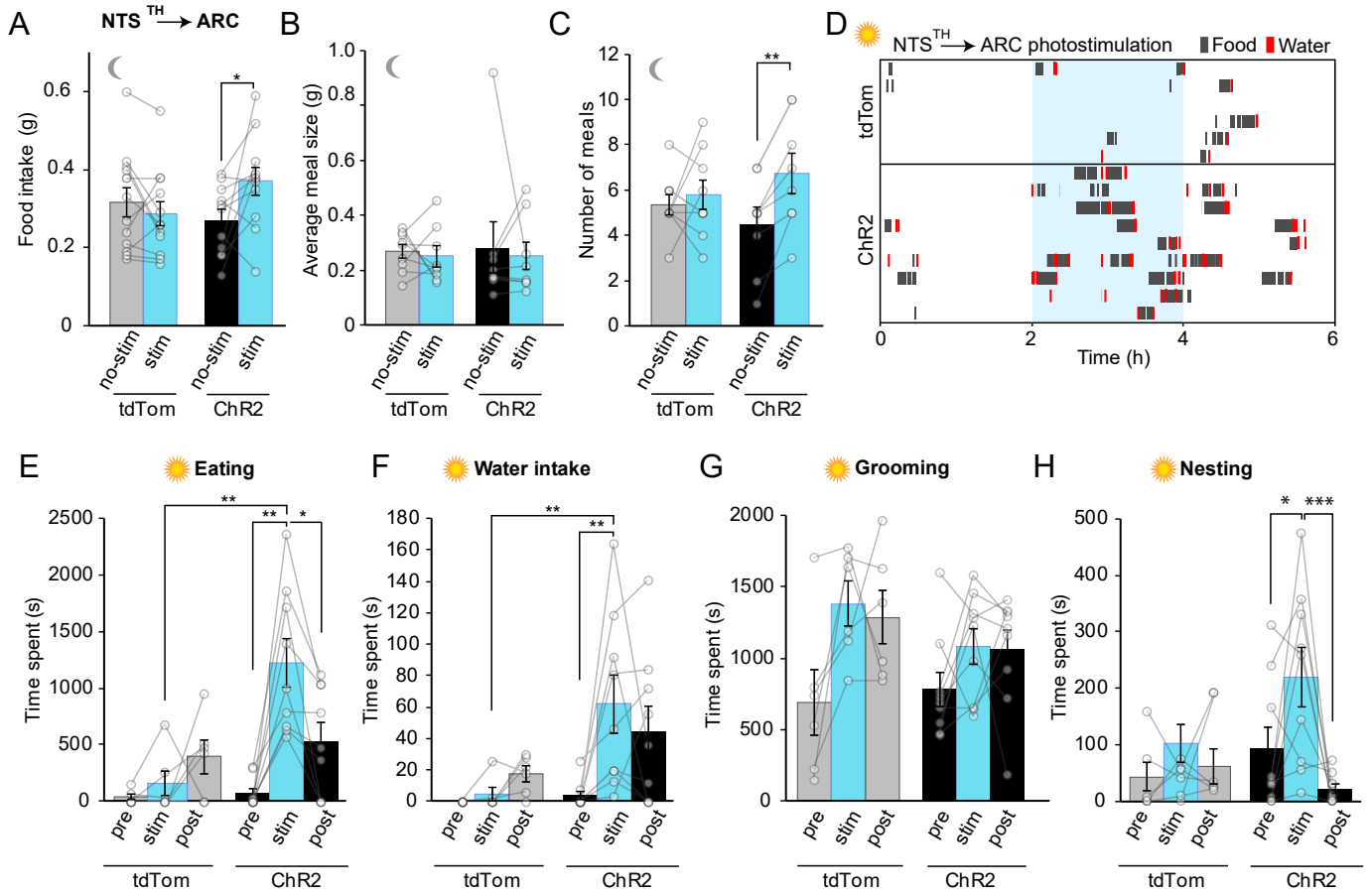


**Figure S2. Behavioral analysis of NTS$^{TH}$→ARC axonal stimulation** (related to Figure 2).

(A) Summary graph of dark onset food intake in response to NTS$^{TH:ChR2}$→ARC and NTS$^{TH:tdTom}$→ARC axonal photostimulation in *ad libitum*-fed mice. Each bar represents 1 hour of food intake (n = 12 tdTomato mice, n = 11 ChR2 mice, RM two-way ANOVA interaction F(1,21) = 6.507, p = 0.0186, Sidak's corrected p value).

(B-C) Impact of NTS$^{TH:ChR2}$→ARC and NTS$^{TH:tdTom}$→ARC axonal photostimulation on meal pattern parameters of ad *libitum-fed* mice in dark onset. (B) Average meal size and (C) total number of meals. Each bar represents feeding data (4 hours) on non-stimulated days (gray or black bars), or stimulated days (blue bars) on the same time period of dark cycle (n = 9 tdTomato mice, n = 8 ChR2 mice, RM two-way ANOVA, interaction (meal size, B): (F1,15) = 0.01029, p= 0.925; stim (number of meals, C): F(1,15) = 9.276, p = 0.0082, Sidak's corrected p values).

(D) Raster plot of time spent on feeding and drinking in response to NTS$^{TH:ChR2}$→ARC and NTS$^{TH:tdTom}$→ARC axonal photostimulation in *ad libitum*-fed mice during day. Each row represents an individual mouse. Time spent on feeding is marked in grey and drinking in red; blue shade represents the stimulation time frame.

(E-H) Impact of NTS$^{TH:ChR2}$→ARC and NTS$^{TH:tdTom}$→ARC axonal photostimulation on time spent for various behavioral parameters: eating (E) and water intake (F), and on home cage activities, grooming (G) and nesting (H), in *ad libitum*-fed mice during day (n= 6 tdTomato mice, n=9 ChR2 mice, two way RM ANOVA, interaction (eating, E): F(2,26) = 9.101, p = 0.0010; stim (water, F): F(2,26) = 4.857, p = 0.0161; interaction (grooming, G): F(2,26) = 0.9450, p = 0.4016; stim (nesting, H): F(2,26) = 5.555, p = 0.0098. Tukey corrected p-values).

Data are expressed as mean ± SEM. *p < 0.05, **p < 0.01, ***p < 0.001

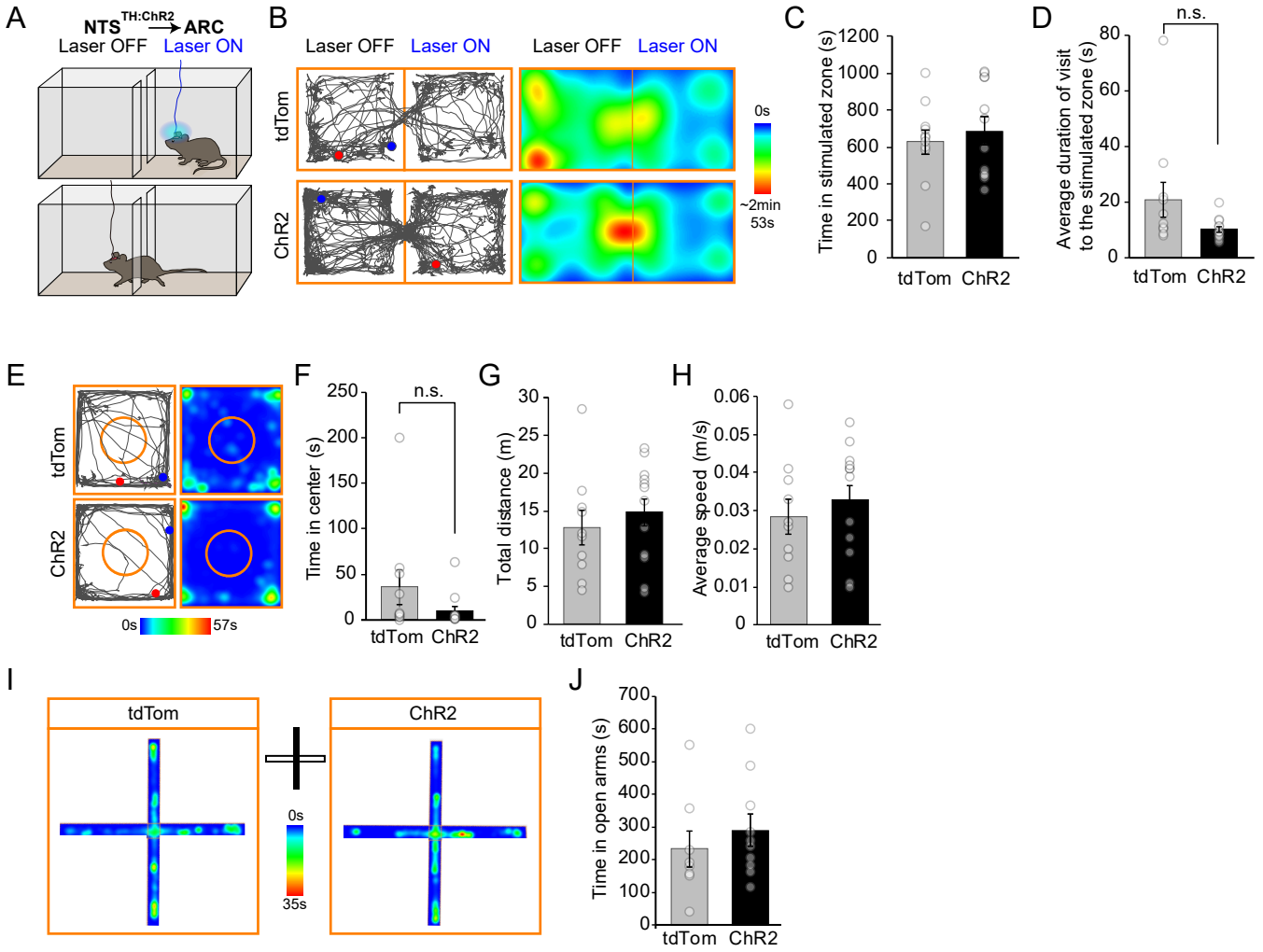


**Figure S3. Evaluation of anxiolytic and valence features of NTS$^{TH}$→ARC axonal stimulation** (related to Figure 2).

(A-D) Active place preference assay. Schematic diagram describing the active place preference assay (A). NTS$^{TH}$→ARC axonal stimulation was applied while mice were in one side of the chamber (stimulated zone) and were not stimulated in the other side (n = 11 tdTomato mice, n = 12 ChR2 mice). Representative tracks (left) and mean heatmaps (right) generated during the 30 min protocol (B). Total time spent in (C), and the average duration of each visit (D) to the stimulated zone were similar in mice expressing ChR2 and tdTomato in NTS$^{TH}$ neurons (unpaired t-test). Blue and red spots represent track starting and ending points respectively.

(E-H) Open field test during NTS$^{TH}$→ARC axonal stimulation (n = 10 tdTomato mice, n = 12 ChR2 mice). Representative tracks (left) and mean heatmaps (right) generated during the 10 min protocol (E). Time spent in the center zone (inside circle, F), total distance achieved (G), and average speed of the mice (H) were not significantly different between ChR2 and tdTomato groups (unpaired t-test). Blue and red spots represent track starting and ending points respectively.

(I-J) Elevated plus maze assay during NTS$^{TH}$→ARC axonal stimulation (n= 8 tdTomato mice, n= 10 ChR2 mice). Mean heatmaps for each group are shown (I). Time spent in the open arms was similar between tdTomato and ChR2 mice (unpaired t-test).

n.s.: not significant; data are expressed as mean ± SEM.

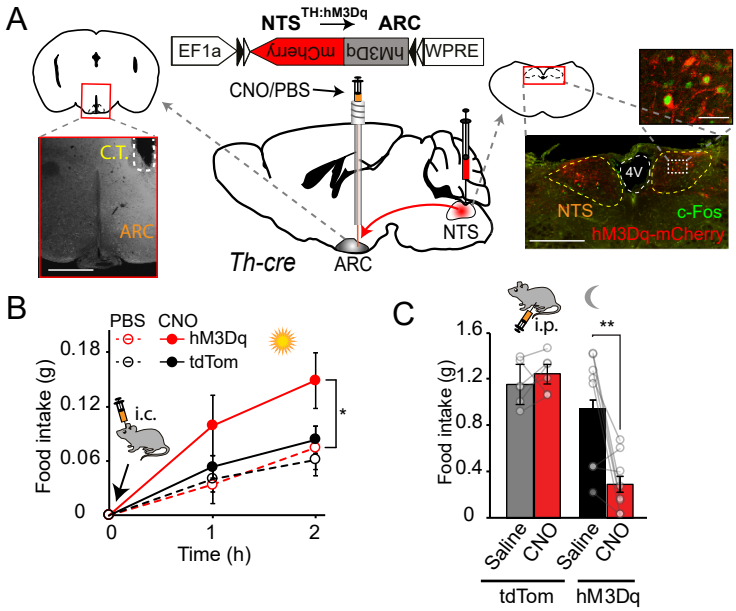


**Figure S4. Opposite effects of global chemogenetic activation of entire NTS$^{TH}$ neurons versus local activation of NTS$^{TH}$→ARC projections** (related to Figure 2 and Figure 7).

(A) Schematic and representative images of targeted hM3Dq-mCherry expression in NTS$^{TH}$ neurons of *Th-cre* mice. Left: Schematic and representative photomicrograph showing ARC implanted with cannula tract (C.T., outlined by dashed line). Scale bar: 500 μm. Middle: Schematic of cre-dependent hM3Dq expressing virus injection and cannula placement. Right: Schematic and representative photomicrographs showing transduced TH neurons expressing hM3Dq-mCherry (red) and c-Fos staining (green) in NTS (outlined by dashed line). Scale bars: 500 μm and 50 μm.

(B) Summary graph for cumulative food intake depicting the impact of intra-ARC (i.c.) injection of CNO (solid lines) versus PBS (dashed lines) in *ad libitum*-fed hM3Dq (red circles) or control mice (tdTomato, black circles) during light cycle (n = 9 control (tdTomato) mice, n = 9 hM3Dq mice; two-way RM ANOVA, treatment ($F_{5,80}$): 15.47, $p < 0.0001$, Tukey corrected p value).

(C) Summary graph for food intake depicting appetite suppression in *ad libitum* fed mice at dark onset upon global NTS$^{TH}$:hM3Dq activation by intraperitoneal (i.p.) CNO delivery (n = 8 hM3Dq, n= 6 tdTomato mice, 4 hours food intake, two-way RM ANOVA interaction: $F_{1,12} = 23.94$, $p = 0.0004$, Sidak's corrected p values).

Data are expressed as mean ± SEM. *p<0.05, **p<0.01

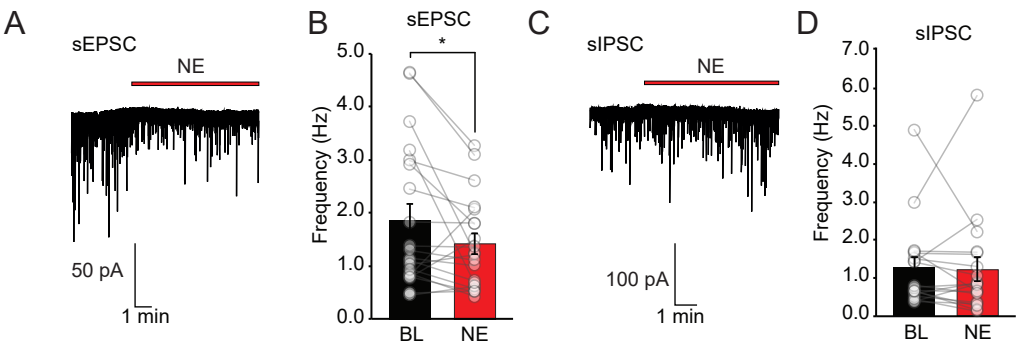


**Figure S5. Norepinephrine (NE) does not stimulate glutamatergic synaptic drive onto AgRP neurons** (related to Figure 6).

(A and B) Representative traces and summary graph for the impact of bath applied NE (10 μM) on sEPSC recorded from AgRP neurons in *Npy-gfp* mice (n = 20 neurons, paired t-test, p = 0.0407).

(C and D) Representative traces and summary graph for the impact of bath applied NE on sIPSC recorded from AgRP neurons in *Npy-gfp* mice (n = 18 neurons paired t-test, p = 0.78).

Data are expressed as mean ± SEM. *p<0.05, BL: Baseline

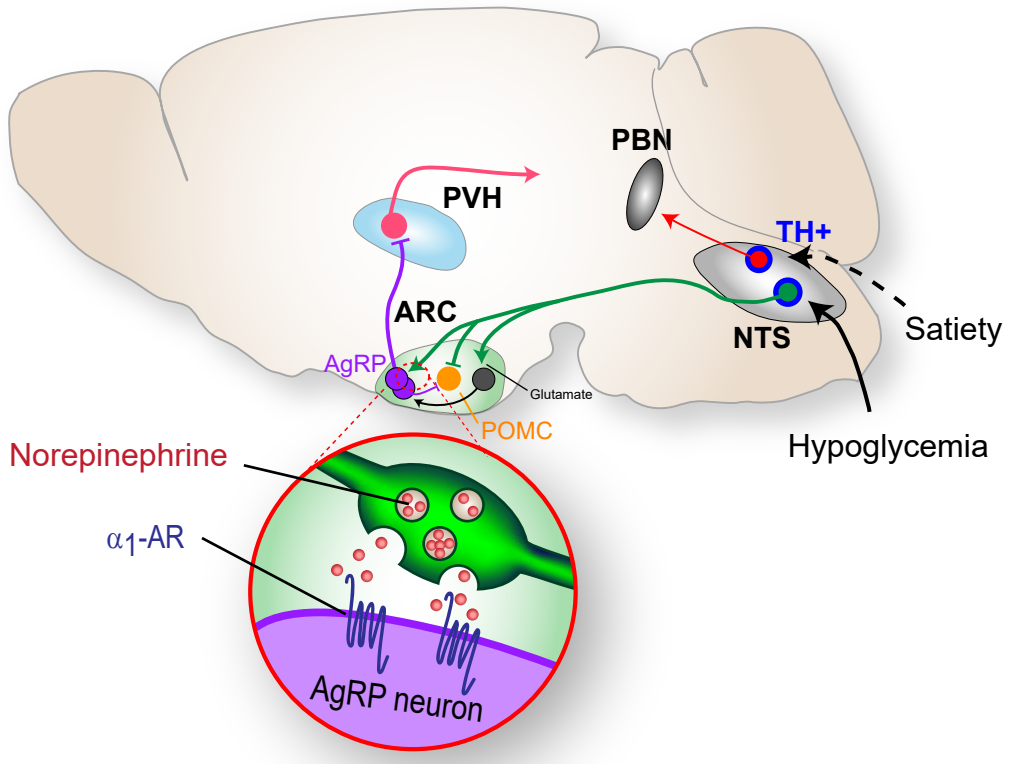


**Figure S6. Hypothalamic targets of NTS catecholamine neurons in glucoprivic feeding** (related to Figures 1-7).

Summary model for the circuitry engaged by ascending $NTS^{TH}$ axons in the ARC.